

Supporting information

Multimode Crawling Motions of Azobenzene Crystal Induced by Light Intensities for Application as a Shape-Changeable Microcleaner

**Makoto Saikawa,^{ab} Kengo Manabe,^b Koichiro Saito,^b
Yoshihiro Kikkawa^b and Yasuo Norikane^{*bc}**

^a Graduate School of Science and Technology, University of Tsukuba,
Tsukuba, Ibaraki 305-8571, Japan

^b Research Institute for Advanced Electronics and Photonics,
National Institute of Advanced Industrial Science and Technology (AIST),
Tsukuba, Ibaraki 305-8565, Japan

^c Faculty of Pure and Applied Sciences, University of Tsukuba,
Tsukuba, Ibaraki 305-8571, Japan

*Corresponding Author. E-mail: y-norikane@aist.go.jp

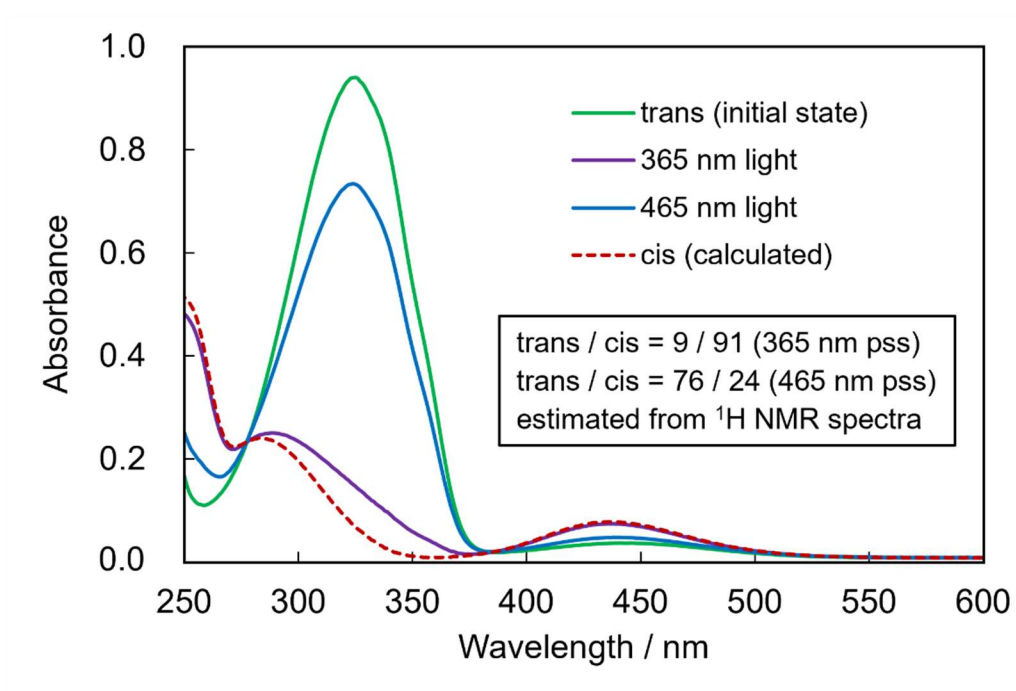


Figure S1. Absorption spectra of DMAB (50 μM in chloroform). The *cis* isomer is dominant (91% estimated from ¹H NMR spectra) upon irradiation with 365 nm LED, whereas the *trans* isomer is dominant (76% estimated from ¹H NMR spectra) upon irradiation with 465 nm LED.

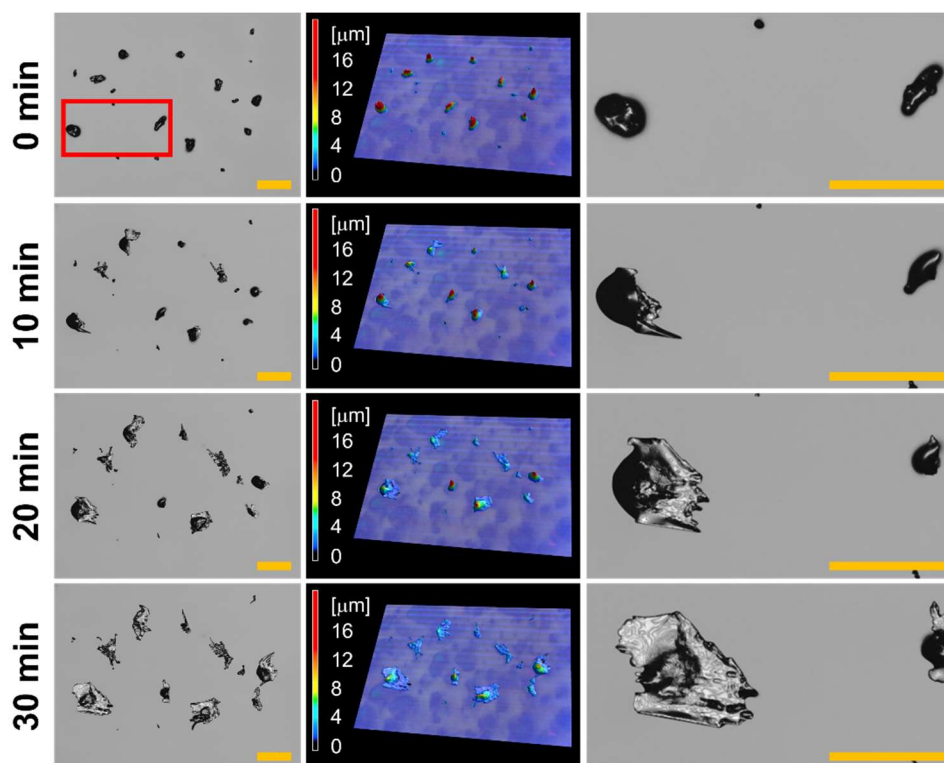


Figure S2. Photomicrographs of the crawling motion of DMAB crystals on the Hyb10 film after irradiation for $t = 0, 10, 20,$ and 30 min. The first column presents the photomicrographs of the entire field of view, second column shows 3D images obtained by using a laser scanning microscope, and third column depicts enlarged images of the square in the first column. Light irradiation was performed from the left for UV (365 nm) light and from the right for visible (465 nm) light. The intensities of 365 and 465 nm were 200 and 200 mW cm^{-2} , respectively. Scale bar: $100 \text{ }\mu\text{m}$.

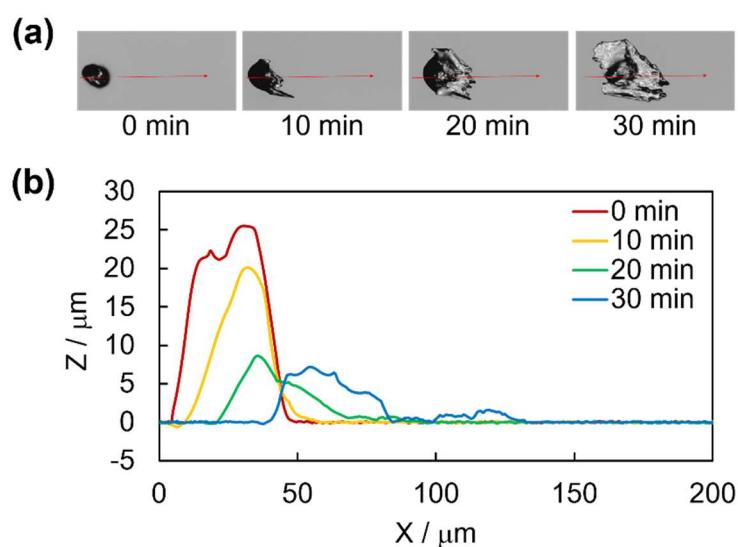


Figure S3. Height profiles of crawling DMAB crystals on the Hyb10 film observed by using a laser scanning microscope. (a) Photomicrographs of DMAB crystals on the Hyb10 film after irradiation for $t = 0, 10, 20,$ and 30 min. (b) Height profiles of the DMAB crystals along the red arrow in (a) after irradiation for $t = 0, 10, 20,$ and 30 min. Light irradiation was performed from the left for UV (365 nm) light and from the right for visible (465 nm) light. The intensities of 365 and 465 nm were 200 and 200 mW cm^{-2} , respectively.

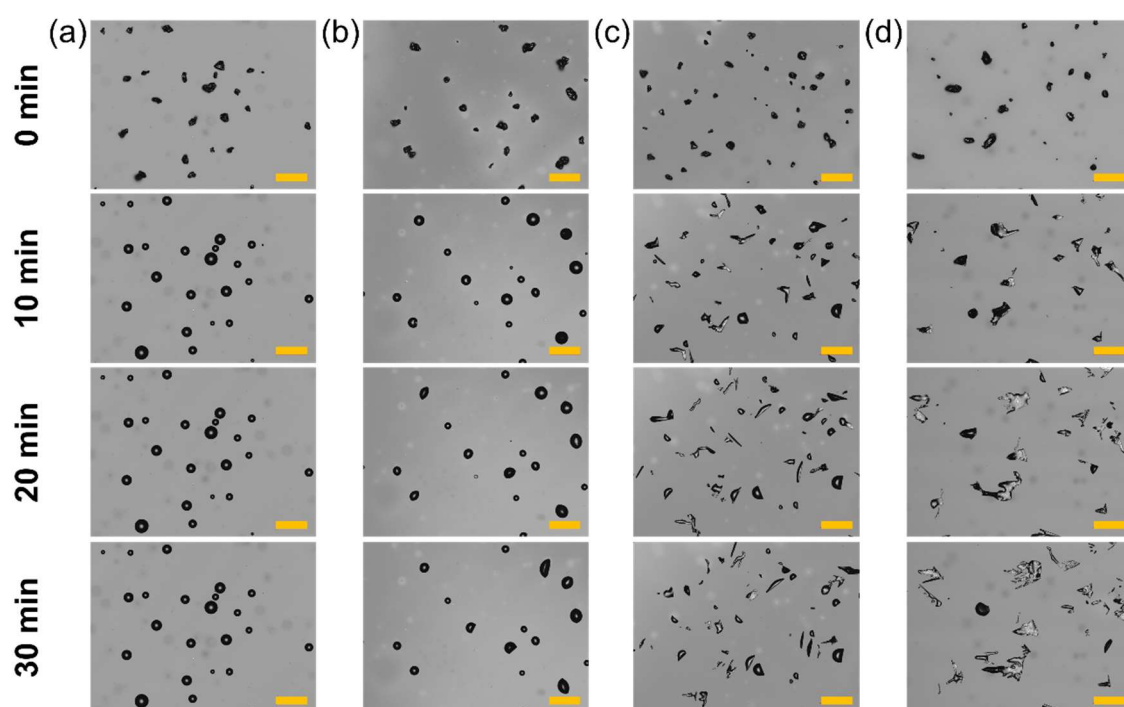


Figure S4. Photomicrographs of the crawling motion of DMAB crystals on the Hyb10 film after irradiation for $t = 0, 10, 20,$ and 30 min. The intensities of 365 and 465 nm were (a) 200 and 0 mW cm^{-2} , (b) 200 and 20 mW cm^{-2} , (c) 200 and 100 mW cm^{-2} , and (d) 200 and 150 mW cm^{-2} . Light irradiation was performed from the left for UV (365 nm) light and from the right for visible (465 nm) light. Scale bar: 100 μm .

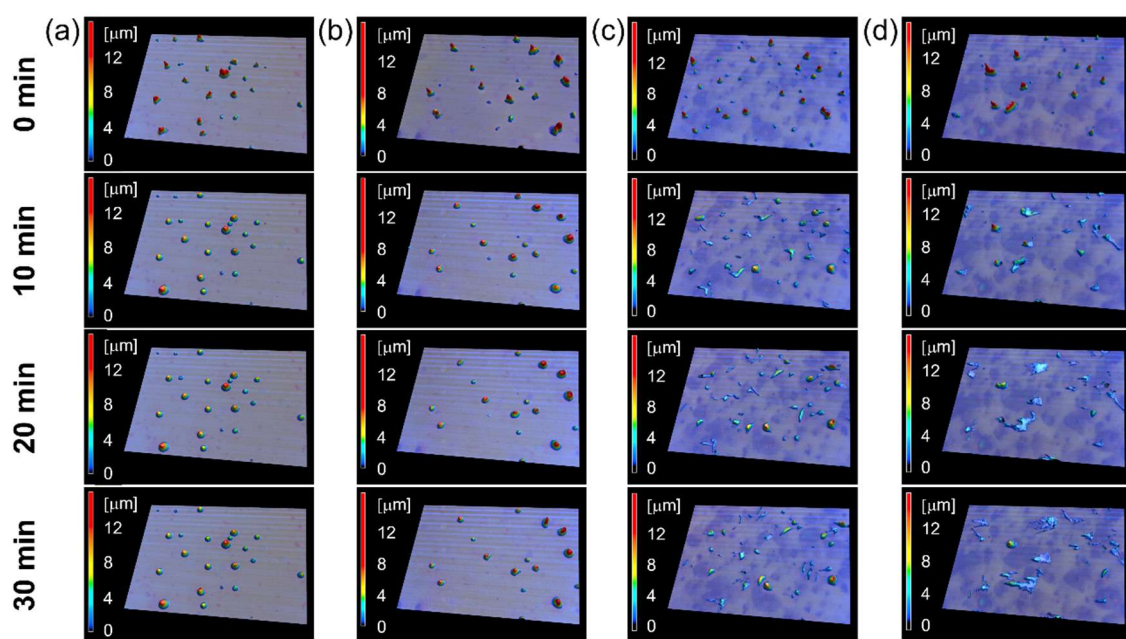


Figure S5. 3D images of the crawling motion of DMAB crystals on the Hyb10 film obtained by using a laser scanning microscope after irradiation for $t = 0, 10, 20,$ and 30 min. The intensities of 365 and 465 nm were (a) 200 and 0 mW cm^{-2} , (b) 200 and 20 mW cm^{-2} , (c) 200 and 100 mW cm^{-2} , and (d) 200 and 150 mW cm^{-2} . Light irradiation was performed from the left for UV (365 nm) light and from the right for visible (465 nm) light.

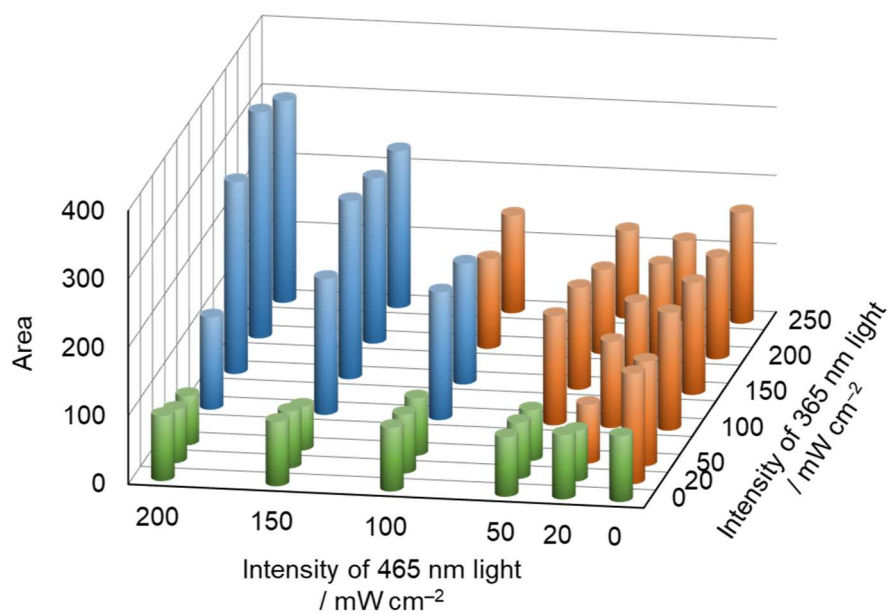


Figure S6. Relative average area of DMAB crystals, projected onto the substrate surface with the initial crystal area set to 100, against irradiation intensities after irradiation for 30 min on the Hyb10 film. The color of each bar (blue, orange, or green) corresponds to the physical attributes indicated in the photomicrographs in Figure 3.

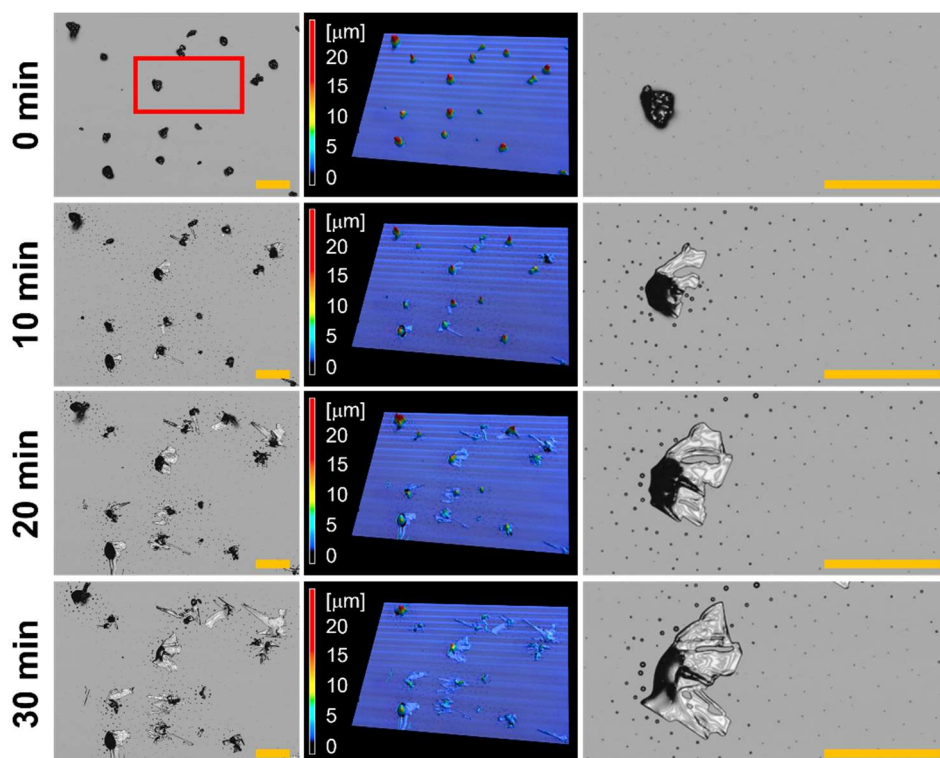


Figure S7. Photomicrographs of the crawling motion of DMAB crystals on the TMS10 film after irradiation for $t = 0, 10, 20,$ and 30 min. The first column presents the photomicrographs of the entire field of view, second column shows 3D images obtained by using a laser scanning microscope, and third column depicts enlarged images of the square in the first column. Light irradiation was performed from the left for UV (365 nm) light and from the right for visible (465 nm) light. The intensities of 365 and 465 nm were 200 and 50 mW cm^{-2} , respectively. Scale bar: 100 μm .

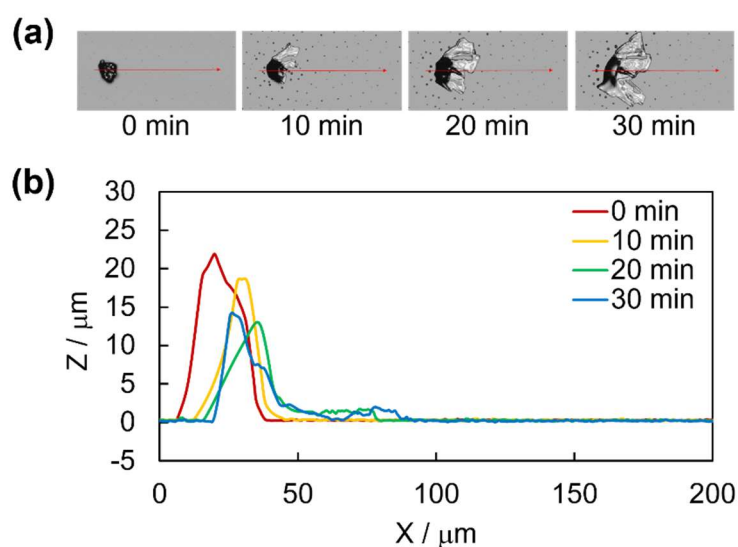


Figure S8. Height profiles of crawling DMAB crystals on the TMS10 film observed by using a laser scanning microscope. (a) Photomicrographs of DMAB crystals on the TMS10 film after irradiation for $t = 0, 10, 20,$ and 30 min. (b) Height profiles of the DMAB crystals along the red arrow in (a) after irradiation for $t = 0, 10, 20,$ and 30 min. Light irradiation was performed from the left for UV (365 nm) light and from the right for visible (465 nm) light. The intensities of 365 and 465 nm were 200 and 200 mW cm^{-2} , respectively.

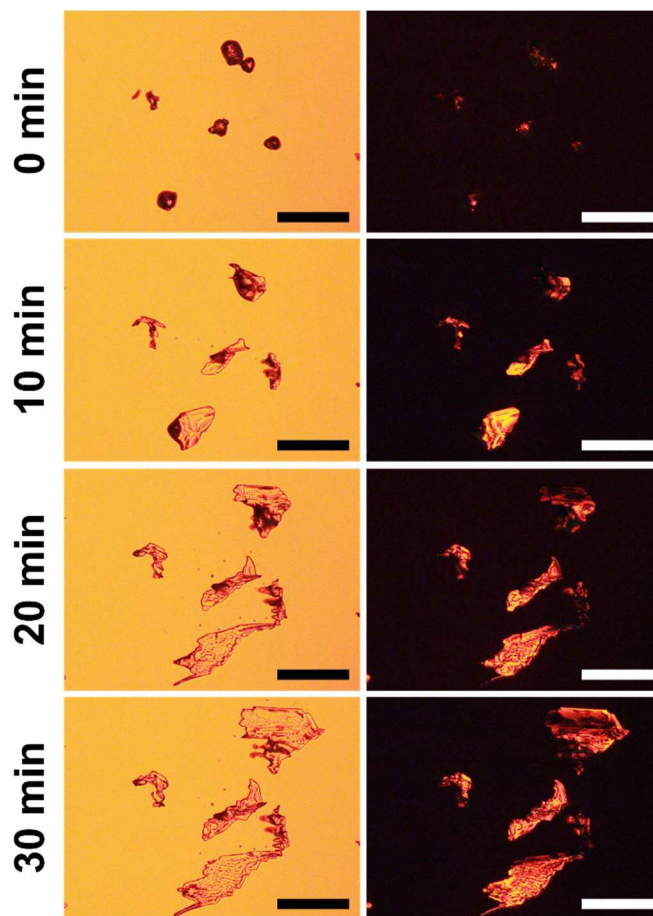


Figure S9. Photomicrographs of the crawling motion of DMAB crystals on the Hyb10 film after irradiation for $t = 0, 10, 20,$ and 30 min. The first column presents photomicrographs under bright-field, and the second column shows photomicrographs under polarizing optical microscopes with crossed-polarizer orientation. Light irradiation was performed from the left for UV (365 nm) light and from the right for visible (465 nm) light. The intensities of 365 and 465 nm were 200 and 200 mW cm^{-2} , respectively. Scale bar: $100 \mu\text{m}$.

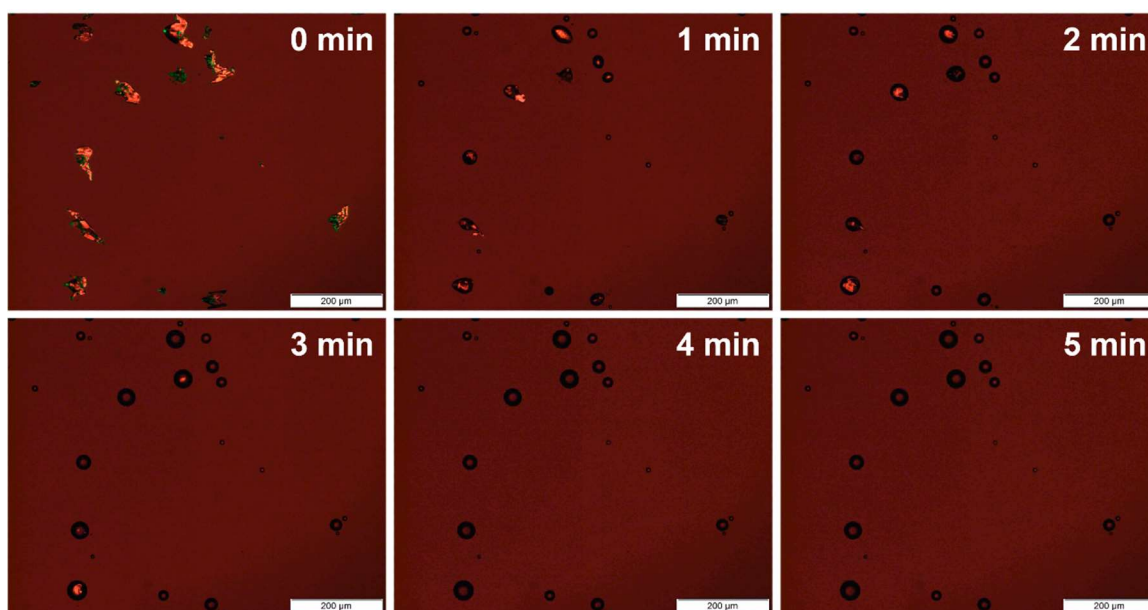


Figure S10. Photomicrographs of transformation of DMAB crystals under polarizing optical microscopes with a fixed polarizer angle at 10° on the Hyb10 film after irradiation under condition 2 for $t = 0, 1, 2, 3, 4,$ and 5 min. The photomicrograph at 0 min shows the DMAB crystals after exposure under condition 1 for 20 min. Condition 1: 365 and 465 nm (200 and 200 mW cm^{-2}). Condition 2: 365 nm (200 mW cm^{-2}). Light irradiation was performed from the left for UV (365 nm) light and from the right for visible (465 nm) light. Scale bar: 200 μm .

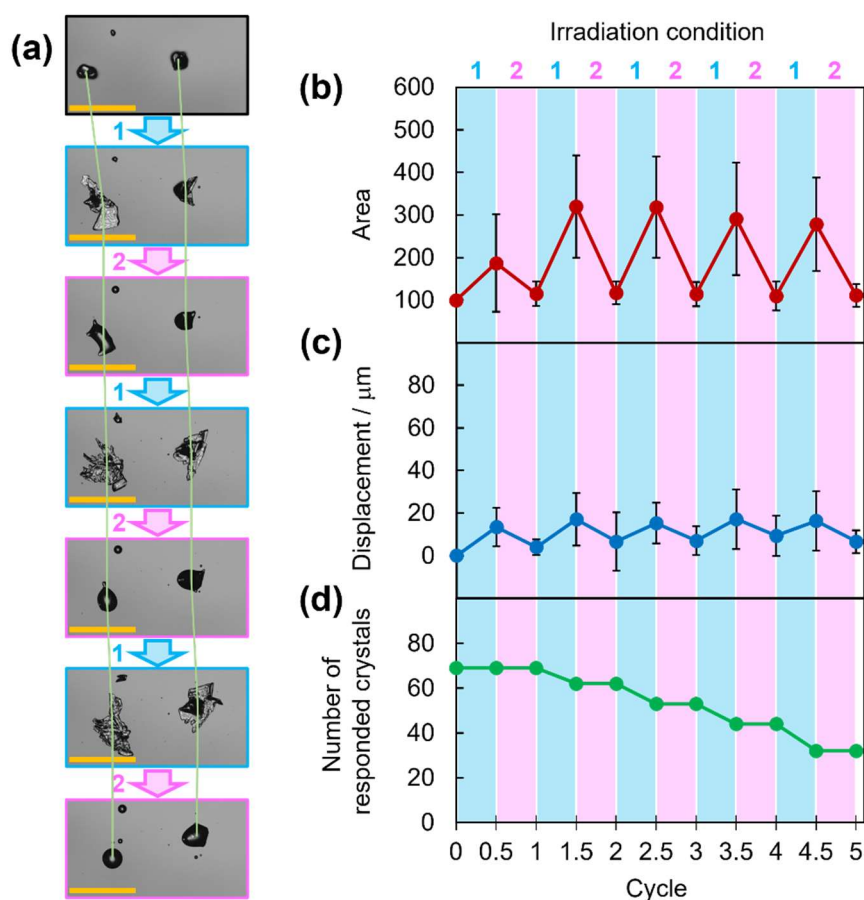


Figure S11. (a) Photomicrographs of the crawling motion and deformation of DMAB crystals on the Hyb10 film under alternating irradiation conditions. Scale bar: 100 μm . Condition 1: 365 and 465 nm (200 and 200 mW cm^{-2}) of UV and visible light, respectively, for 20 min. Condition 2: 365 nm UV light (200 mW cm^{-2}) for 2 min. Light irradiation was performed from the left for UV (365 nm) light and from the right for visible (465 nm) light. Changes in (b) area, (c) displacement, and (d) number of responded crystals.

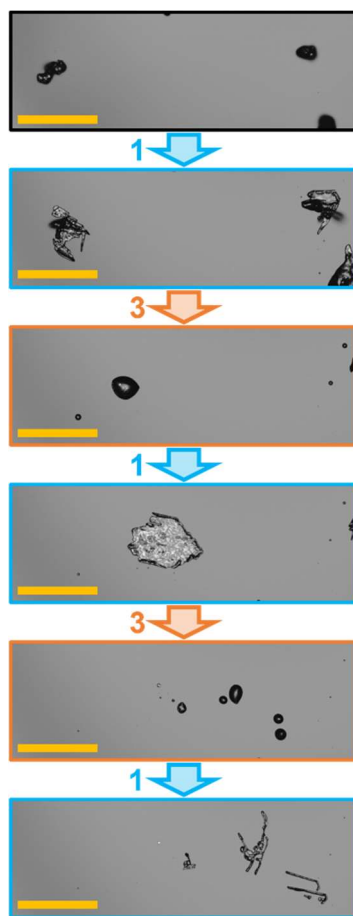


Figure S12. Photomicrographs of the crawling motion and deformation of DMAB crystals on the Hyb10 film under alternating irradiation conditions. Condition 1: 365 and 465 nm (200 and 200 mW cm^{-2}) for 20 min. Condition 3: 365 and 465 nm (200 and 50 mW cm^{-2}) for 20 min. Light irradiation was performed from the left for UV (365 nm) light and from the right for visible (465 nm) light. Scale bar: $100 \mu\text{m}$.

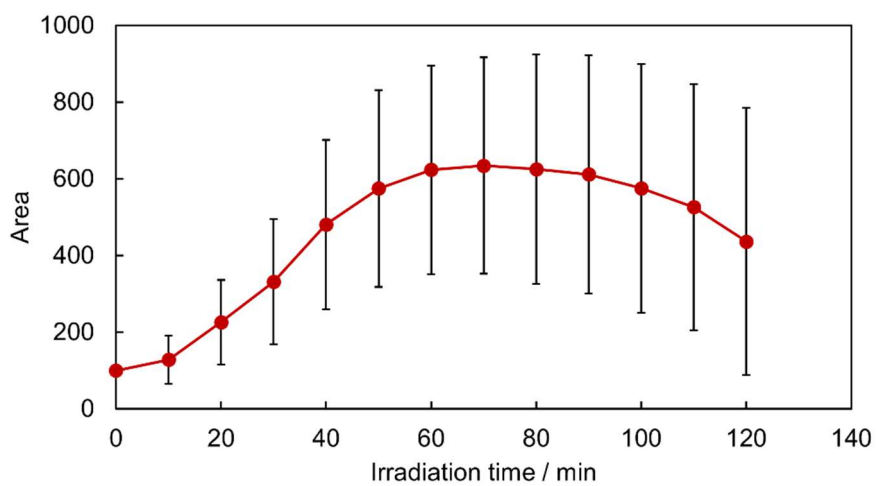


Figure S13. Relative average area of DMAB crystals, projected onto the substrate surface with the initial crystal area set to 100, after light irradiation for every 10 minutes on the Hyb10 film. The intensities of 365 and 465 nm were 200 and 200 mW cm^{-2} , respectively.

Supplementary movies

Movie S1. Crawling motion of DMAB crystals on the Hyb10 film (UV (365 nm)–visible (465 nm) = 200–200 mW cm⁻²).

Movie S2. Crawling motion of DMAB crystals on the TMS10 film (UV (365 nm)–visible (465 nm) = 200–200 mW cm⁻²).

Movie S3. Transformation of DMAB crystals from spread shape to droplet-like shape.

Movie S4. Cycle of irradiation condition 1, 2, 3, and 2.

Movie S5. Cycle of irradiation condition 1 and 2.

Movie S6. Cycle of irradiation condition 1 and 3.

Movie S7. Demonstration of a shape-changeable microcleaner.